Clays and Clay Minerals, Vol. 64, No. 3, 210–219, 2016.

THE INFLUENCE OF HIGH-CONCENTRATION Na HEXAMETAPHOSPHATE DISPERSANT ON THE RHEOLOGICAL BEHAVIOR OF AQUEOUS KAOLIN DISPERSIONS

Francisco-José Rubio-Hernández[1,2,*], Nicolás-Marcelo Páez-Flor[1], Ana-Isabel Gómez-Merino[2], Francisco-José Sánchez-Luque[2], Reinaldo Delgado-García[1], and Leonardo Goyos-Pérez[1]

[1] DECEM, Universidad de las Fuerzas Armadas, Sangolquí, Ecuador
[2] Departamento de Física Aplicada II, Universidad de Málaga, Spain

Abstract—Previous studies of dispersant–aqueous kaolin dispersions have indicated clearly that the concentration of the dispersant determines the type of rheological behavior. Those studies focused on the use of dispersant concentrations below the limit of saturation, ignoring what might have happened at concentrations above that limit, and the practical uses to which such information might be put. The present study examined the influence of sodium hexametaphosphate dispersant on the viscous and viscoelastic properties of aqueous kaolin dispersions when its concentration was greater than the saturation limit. A concentric-cylinders geometry sensor system (with a narrow gap between the cylinders) was used to test the rheological behavior of Na hexametaphosphate-aqueous kaolin dispersions. Aqueous kaolin dispersions were viscoplastic, thixotropic, and viscoelastic fluids. The analysis of frequency sweep tests in the linear viscoelastic limit and steady-flow curves led to the conclusion that an increase in the dispersant concentration above the limit of saturation gave way to 'solid-like' dispersions.

Key Words—Kaolin Dispersions, Na Hexametaphosphate, Rheology.

INTRODUCTION

Kaolin is one of the most widely used clay minerals in industrial applications (Murray, 2000). When peptized (Van Olphen, 1963), the dispersions of kaolin particles are used for specific applications, *e.g.* in the production of high-performance ceramics or paper coatings (Murray, 1961). Two main features determine optimum performance in the peptized state. First, good results are obtained only if the dispersions are homogeneous and stable (Le Bell *et al.*, 1976; Choi *et al.*, 1993). Second, the optimum development of an industrial process is achieved only if the specific response of the kaolin dispersions to mechanical stresses is well characterized (Papo *et al.*, 2002). In other words, optimum performance of peptized kaolin dispersions is determined by their homogeneity, stability, and rheology.

As a general rule, dispersions are assumed to be homogeneous when their components are macroscopically indistinguishable. On the other hand, dispersions are considered to be stable against particle sedimentation when they maintain homogeneity consistently (Hunter, 1981). The use of dispersants improves both attributes (Kronberg *et al.*, 1986) and is necessary specifically when the concentration of particles is great (Sjöberg *et al.*, 1999; Bergaya *et al.*, 2006). This is because the dispersants adsorbed onto the particle surface induce a double repulsion mechanism between particles: electrostatic (Eygi and Atesok, 2008) and steric (Konan *et al.*, 2008) repulsion. This repulsive potential energy reduces the formation of particle aggregates, favoring the homogeneity of the dispersion and preventing sedimentation of the solid phase.

Polyphosphates are the most commonly used dispersants in the kaolin industry, but silicates and polycarboxylates are also used sometimes. Silicates have shown a limited effectiveness for kaolin dispersions (Ma, 2011) because the stabilization of the silicate-kaolin system was controlled mainly by electrostatic interactions, whereas the polycarboxylates and polyphosphates have demonstrated much greater ability to remain homogeneous and stabilize the aqueous kaolin dispersions, which is because of both electrostatic and steric repulsion between kaolin particles (Papo *et al.*, 2002; Eygi and Atesok, 2008; Li *et al.*, 2014). Owing to their greater concentration effect on the rheology of the dispersant-kaolin system, only the polyphosphates were considered in the present study.

Increasing the abundance of dispersed particles in Newtonian fluids results in a variety of non-Newtonian flow behaviors (Mewis and Spaull, 1976). These non-Newtonian behaviors are influenced by several parameters including the particle concentration, the pH of the liquid medium, the duration of the mechanical action, the type, size, and shape of the particles, and the level of aggregation (Tombácz and Szekeres, 2006; Loginov *et al.*, 2008). Proper rheological studies on paper coating (Triantafillopoulos, 1996) and on kaolin aqueous suspensions peptized with Na hexametaphosphate (NaHMP) (Papo *et al.*, 2002; Andreola *et al.*, 2006) are rare. Papo *et al.* (2002) observed that shear-thinning behavior in 55 wt.% aqueous kaolin dispersions changed to shear-

* E-mail address of corresponding author:
fjrubio@uma.es
DOI: 10.1346/CCMN.2016.0640301

https://doi.org/10.1346/CCMN.2016.0640301 Published online by Cambridge University Press

Table 1. Chemical composition of the kaolin (wt.%, determined by the supplier using XRF).

SiO_2	Al_2O_3	K_2O	Fe_2O_3	MgO	CaO	Na_2O	TiO_2	Others
47.0	36.5	1.6	1.1	0.2	0.1	0.1	0.1	12.8

thickening behavior when the NaHMP concentration in the aqueous kaolin dispersion was fixed in the interval 0.045−0.005 wt.%. Such viscous, time-independent behavior was explained by assuming steric interaction between polyphosphate chains linked to particle surfaces, giving way to non-flocculated dispersions in that interval of dispersant concentration. Oscillatory tests supported this result (Papo *et al.*, 2002), dispersions being stable when the dispersant concentration varied over the interval 0.100−0.500 wt.%; however, they observed shear-thinning behavior above the adsorption saturation limit (of 0.500 wt.%) of the dispersant. They further explained that the transition from shear-thickening to shear-thinning behavior at NaHMP concentrations >0.500 wt.% resulted from an excess of dispersant, which caused destabilization, flocculation, and viscosity increase in the suspension. Kaolin-particle alignment and linear orientation of NaHMP molecules in the flow direction were also used as arguments to explain shear-thinning behavior above the adsorption saturation limit of the dispersant (Papo *et al.*, 2002). Those rheological studies suggested clearly that the concentration of NaHMP dispersant is a determining factor in the rheological behavior of the aqueous kaolin dispersions and indicated, as a result, the possibility of different practical applications. In other words, those studies indicated the need to study in greater detail the influence of the concentration of NaHMP dispersant on the rheological behavior of aqueous kaolin dispersions, because specific uses of this product are determined largely by its mechanical behavior. In the present study, continuous and oscillatory shear were applied to concentrated aqueous kaolin dispersions in which kaolin particles had been dispersed with a concentration of the dispersant (NaHMP) of >0.500 wt.%.

EXPERIMENTAL

The kaolin used in the present study (tradename "C35") was supplied by Caolines de Vimianzo, S.A.U. (Spain). This kaolin was obtained from a granite site (Vimianzo, Costa de la Muerte, Galicia, Spain) and tailored by the manufacturer for use in the manufacture of ceramics. Chemical analysis of the kaolin, by Caolines de Vimianzo, S.A.U. (Table 1), was determined by X-ray fluorescence (XRF). The approximate mineralogical composition was: 85−95% kaolinite, 10−15% muscovite, and 2% other minerals. The specific surface area, determined by nitrogen adsorption (BET method), was 18.6±0.1 m^2/g; the mean particle size, obtained from particle-size distribution, was 2 μm; the mean particle thickness, obtained from the (001) X-ray reflection using the Scherrer equation, was 23 nm.

NaHMP (from Sigma-Aldrich Chemical GmbH, Düsseldorf, Germany) was used as the dispersant. The sample preparation was designed to maintain constant kaolin and water+NaHMP concentrations (Table 2). The oven-dried powder was mixed with double-distilled water (>1.0 MΩ cm at 25ºC (type 2), Millipore) and the dispersant in a stirrer RZR1 (Heidolph Instruments, Germany) at 215 rpm ($1.3 \times g$) for 10 min, yielding apparently homogeneous dispersions.

Rheological experiments were carried out at a temperature of 25.0 ± 0.1ºC using a Peltier-controlled temperature system on a Discovery Hybrid Rheometer DHR2 (TA Instruments, USA), using a concentric-cylinder sensor system with a conical bob of 14 mm radius, length of 42 mm, and a cup of 15 mm radius. As the condition of 'small gap' (14/15 > 0.90) was accomplished, samples were sheared under simple shear conditions. Experiments were conducted under steady and oscillatory shear. The absence of a slip wall was checked by comparing the results obtained with different bob lengths immersed in the sample.

To minimize the possible effects of aging of the sample that could influence the results, a portion of each sample was sheared at 50 s^{-1} and the variations in the steady shear-stress value were observed for 30 min. No observable chemical or physical changes in the kaolin/water/dispersant system occurred during this rheological test; as each test lasted <20 min, the results could, therefore, be interpreted as suffering no effects of aging.

To be sure that irreversible microstructural changes were not generated in the samples due to the mechanical action, a reversibility test was applied to all systems before the design of the rheological tests. From a reference shear rate (1 s^{-1}), step-down (0.1 and 0.5 s^{-1}) and step-up (5, 10, 50, 100, 500, 1000 s^{-1})

Table 2. Composition (wt.%) of the aqueous kaolin dispersions.

System	Kaolin	Water	NaHMP
K50D0	50	50	0
K50D01	50	49.9	0.1
K50D05	50	49.5	0.5
K50D1	50	49	1
K50D2	50	48	2

https://doi.org/10.1346/CCMN.2016.0640301 Published online by Cambridge University Press

tests were carried out sequentially, returning each time to the reference shear. The minimal variation (<10%) of the steady shear stress measured at the reference shear rate after each step was assumed to be an indication of the reversibility of the mechanical action. The results confirmed that microstructure changes were reversible when the shear rate was <550 s^{-1}.

To avoid random errors from the rheometer geometry, a pre-shear rate of 50 s^{-1} was applied to the sample for 60 s. The record of the same steady shear stress value at the end of this pre-shear rate was a quantitative indicator that all subsequent rheological tests were carried out on the same physical state of the material. After the pre-shear phase was complete the sample rested for 30 s. Rest time restored the sample to a certain structural level and this was confirmed as the maximum structural level the sample could achieve because rest-time intervals of >30 s failed to establish any stronger structure. This was quantified by measuring the initial shear stress when the sample was sheared at a low shear rate (1 s^{-1}) after rest during an increasing time interval. The initial shear stress at 1 s^{-1} increased with rest time, but for rest times >30 s, the initial shear stress did not increase further, an indication that the maximum microstructure had been reached.

Non-Newtonian behavior is generally classified into two categories: purely viscous and viscoelastic. Viscous behavior is also divided into time-independent and time-dependent (Barnes *et al.*, 1989). Shear-thinning, shear-thickening, and viscoplasticity belong to the time-independent group. These rheological behaviors are characterized using plots of steady shear stress (τ) *vs.* shear rate ($\dot{\gamma}$), which are referred to as steady-flow curves or rheograms. From a practical point of view, the steady-flow curve is used to predict the flow behavior of a material during industrial processes and other specific applications.

Thixotropy is the purely viscous, time-dependent, rheological behavior which can be characterized by means of the hysteresis or thixotropic loop. This rheological test was accomplished by applying continuously increasing shear rates until a pre-selected maximum shear rate was reached. The sample was sheared at this maximum shear rate until the microstructure achieved the state of maximum break. This process was followed by a decreasing ramp passing through the same shear-rate values during the same time interval as with the increasing ramp. Break-down and build-up processes of micro-structures evolve at different rates if differences exist between the up and down (non-steady) flow.

Materials that show simultaneously viscous and elastic characteristics exhibit viscoelastic behavior. An oscillatory or dynamic shear test is the most appropriate to determine the viscous and elastic components of a viscoelastic flow. If the amplitude of the oscillatory deformation is small enough (small-amplitude oscillatory shear or SAOS) the response of the material is linear and material functions can be defined. To determine the amplitude range for the linear response of the material, an amplitude sweep test is applied to the sample. Once an amplitude value corresponding to the linear viscoelastic region is selected, a frequency sweep will show the material behavior at short and long time intervals for the experiment.

RESULTS AND DISCUSSION

Steady shear viscous behavior

The steady-flow curve is a graphical representation of the shear stress for different shear rates. Steady state for each shear rate was assumed in the present study when shear stress varied by <5%, *i.e.* ($\frac{d\tau(t)}{dt} \leqslant 0.05$) for 20 s.

Once the experimental conditions for the steady-flow curve were defined and after the pre-shear/rest protocol was applied, each sample was subjected to an increasing series of discrete values of shear rate. The experimental points (Figure 1) were the average of three different measurements, although the error bars were eliminated for clarity. In any case, the standard deviation was <10%. All materials showed viscoplastic behavior independent of the amount of dispersant added to the aqueous kaolin dispersion. Such behavior of aqueous kaolin dispersions stabilized with NaHMP dispersant has not been described specifically in the past (Papo *et al.*, 2002; Andreola *et al.*, 2006) despite the important role that the yield-stress value plays in industrial applications.

Before fitting a viscoplastic model to the experimental data shown in Figure 1, some considerations should be made. A correct viscoplastic model should provide a positive yield stress and a positive linear coefficient and, in addition, all of the model parameters should have fixed dimensions and some physical meaning (Feys *et al.*, 2007). Bingham,

$$\tau = \tau_B + \eta_p \dot{\gamma} \quad (1)$$

and Herschel-Bulkley,

$$\tau = \tau_{HB} + K\dot{\gamma}^n \quad (2)$$

are the most widely used viscoplastic models for fitting steady-flow experimental data. In equations 1 and 2, τ_B and τ_{HB} are the respective yield-stress values, η_p is the plastic viscosity, n is the flow index, and K is the consistency (Herschel-Bulkley: coincides with the viscosity when $n = 1$ but not when $n \neq 1$) of the material. These two models have the following shortcomings, according to analysis by Feys *et al.* (2007). Bingham's model is only applicable when η *vs.* $\dot{\gamma}$ dependence is linear (Barnes, 1999). The Herschel-Bulkley model is applicable to non-linear viscoplastic behavior but contains the parameter K. Although K shows a certain resemblance to the viscosity, physical interpretation is difficult due to its 'unusual' units (Pa s^n). So, comparing the consistencies (K) of two different materials is

https://doi.org/10.1346/CCMN.2016.0640301 Published online by Cambridge University Press

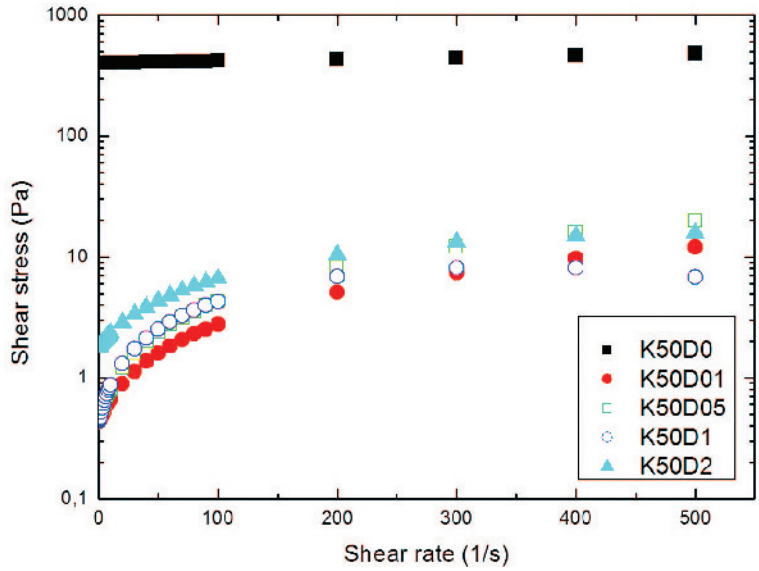

Figure 1. Steady-flow curves of the samples with dispersant. An evolution from linear to non-linear viscoplastic behavior was observed when the dispersant content was >1 wt.%.

generally impossible because the flow indexes (n) will probably be very different. In spite of this, the consistency of materials with different flow indexes have been compared by others (*e.g.* Ouari *et al.*, 2011; Kwak *et al.*, 2015). As an alternative to fitting the experimental steady-flow data of a viscoplastic material, a modified Bingham's model was used, which was created by the addition of a second-order term (c) to Bingham's model, *i.e.*

$$\tau = \tau_{MB} + \eta_p\dot{\gamma} + c\,\dot{\gamma}^2 \quad (3)$$

This equation fitted experimental results in the present study (Figure 1). Equation 3 also satisfies the three conditions which must be achieved by a visco-plastic model (Feys *et al.*, 2007), *i.e.* it must supply a positive yield stress value, it must have a positive linear term in the shear rate to avoid a zero slope at low shear rates, and all of its parameters must have fixed dimensions, which results in a physical meaning for them.

In the absence of dispersant, the aqueous kaolin dispersion showed linear viscoplastic behavior (Bingham) with a very high yield-stress value; addition of a small amount of dispersant (0.100 wt.%), however, was sufficient to reduce the yield stress by three orders of magnitude. The yield value is a function of the number and strength of the particle–particle linkages and can be considered as a measure of the degree of coagulation of the system at rest (Rand and Melton, 1975).

Another interesting overall change observed as the consequence of the addition of dispersant was its effect on non-linear viscoplastic behavior. The second-order term c added to Bingham's model accounts for non-linearity of viscoplastic behavior. The sign of this second-order coefficient determines the type of non-linear response of the system. An enhanced shear-thinning behavior was observed when $c < 0$. On the other hand, $c > 0$ was measured when the apparent viscosity increased with shear rate (shear-thickening behavior). Non-linear viscoplastic behavior was only observed at greater dispersant concentrations, though it was insignificant (Table 3).

Shear-thinning behavior observed in aqueous kaolin dispersions, *i.e.* the fact that apparent viscosity ($\eta = \tau/\dot{\gamma}$) decreased with shear rate, was explained as follows. At rest, the attractive colloidal forces dominated over the hydrodynamic forces and aggregates of particles were assembled. When the shear rate increased, hydrodynamic forces exerted by the flow field were greater than

Table 3. Modified Bingham model parameters obtained after fitting the data shown in Figure 1.

System	τ_{MB} (Pa)	η_p (Pa s)	c (Pa s^2)	r^2
K50D0	400±10	0.16±0.08	0	0.9888
K50D01	0.43±0.02	0.0233±0.0005	0	0.9907
K50D05	0.44±0.01	0.0388±0.0008	0	0.9999
K50D1	0.43±0.01	0.0452±0.0005	$-(6.2\pm0.5)\times10^{-5}$	0.9948
K50D2	1.8±0.2	0.053±0.007	$-(5\pm3)\times10^{-5}$	0.9970

https://doi.org/10.1346/CCMN.2016.0640301 Published online by Cambridge University Press

colloidal forces and the aggregates of kaolin particles divided into smaller units. This disaggregation of the aggregates gave rise to two effects. First, a release of liquid phase trapped in the aggregates occurred, and, second, the distortion of the flow field due to solid phase suspended in the liquid medium was reduced. Consequently, the apparent viscosity of the system decreased.

The addition of a small concentration of dispersant (0.100 wt.%) caused a large decrease in the apparent viscosity of the kaolin-water dispersion (Figure 1). Increasing the dispersant concentration above the adsorption saturation limit (0.500 wt.%), however, reversed this effect and led to a slight increase in the apparent viscosity. To understand this behavior, one must first remember that the kaolin particles are flat, and they have two types of surface charge – one at the edge surfaces and one at the basal surfaces (Van Olphen, 1963). The basal surfaces are negatively charged. The edge surface charge is pH dependent, originating from the protonation/de-protonation of OH groups at the clay mineral edge, and can be either positive (lower pH) or negative (higher pH). The pH at which this charge becomes zero is known as the isoelectric point (pH_{IEP}). The value of pH_{IEP} obtained in the present study from potentiometric titration of a dilute sample of kaolin-water dispersion was 6.8, a value which agrees with that obtained by other authors (Rand and Melton, 1975; Papo *et al.*, 2002).

The interaction of these charges, *i.e.* like-charge repulsion and opposite-charge attraction, from one particle to the next influences the inter-particle associations. These different modes of association were described by Van Olphen (1964) as edge–edge (EE), edge–face (EF), and face–face (FF), and are affected not only by changes in the pH of the medium but also by the electrolyte concentration (Rand and Melton, 1975). If $pH < pH_{IEP}$, the sign of the edge charge is positive and EF structures are expected to dominate at low ionic strengths because positively charged edges are electrostatically attracted to negatively charged basal surfaces (Schofield and Samson, 1954; Rand and Melton, 1975). When $pH \geqslant pH_{IEP}$ and ionic strength is low, the system is fully coagulated as an EE structure. This coagulated structure evolves to a FF structure when the electrolyte concentration increases (Rand and Melton, 1975). Experimental results were interpreted in accordance with these ideas.

The yield-stress value shown by the suspension without dispersant was very large (400±10 Pa), which confirmed that the system at rest had a significant degree of EF structure (coagulated). Adding a small amount of NaHMP dispersant should promote dispersion by decreasing the edge-to-face attraction. However, the effect on particle–particle interaction of possible variation in pH by the addition of dispersant must be taken into account, because it could even have the opposite effect. Therefore, the pH of the suspensions was measured after adding the dispersant. Interestingly, the pH was almost unchanged in the range of dispersant concentrations studied here (0.100–2.000 wt.%), in agreement with what others have reported (*e.g.* Papo *et al.*, 2002). The dissolution of NaHMP in water causes its dissociation into (HMP) and Na^+ ions. The presence of (HMP) and Na^+ ions in small amounts reduced significantly the yield stress value (from 400 to 0.43 Pa) because, as was suggested above, the electrical double layers that surround kaolin particles compressed and the electrical attraction between the edge of one particle and the face of other diminished. Similar to what happens when an electrolyte is added to kaolin dispersions that are in the isoelectric point (Rand and Melton, 1975), EE association mode was presumably the result when a dispersant concentration of less than the adsorption limit (0.500 wt.%) was added. Greater dispersant concentration gave rise to an adsorption process of (HMP) ions onto the face of kaolin particles (Manfredini *et al.*, 1990). This adsorption process led to a saturation effect on the particle face when they were covered completely with (HMP) ions. The increase in the Na^+ ion concentration in the bulk provoked a shield effect on the negative charges existing on the particle face. This reduced repulsive potential energy between particles until FF coagulation mode was achieved (note the small increase in the yield stress value when dispersant concentration was 2.000 wt.%).

Time-dependent viscous behavior

The viscous-flow behavior of a material can only be characterized properly if both the stationary (time-independent) and transient (time-dependent) responses are known; time-dependent behavior of the aqueous kaolin dispersions were studied also, therefore. The transient mechanical response provides information on how fast or slow a microstructure is generated or destroyed. Time-dependent behavior of the material was characterized by applying an increasing shear rate ramp from 0 to 200 s^{-1} followed by constant shearing for 10 s at 200 s^{-1}. After that shear rate, a decreasing ramp from 200 to 0 s^{-1} was applied. To determine the influence of 'shear acceleration' in the time-evolution of the microstructure, the duration of each shear rate ramp took several values between 5 and 180 s. In this way, information on the relative value of the rates of build-up and break-down of the microstructure could be obtained. Two general types of hysteresis curves were obtained. When shear acceleration was small, suspensions showed single, time-dependent behavior irrespective of the dispersant concentration (Figure 2a). In such a case, up and down curves overlapped at high shear rates due to the weakness of the microstructure and/or the coincidence of break-down and build-up rates (both are dependent on shear rate) at high shear rates. On the other hand, up and down curves did not overlap at high shear rates when shear acceleration was high (Figure 2b). In

https://doi.org/10.1346/CCMN.2016.0640301 Published online by Cambridge University Press

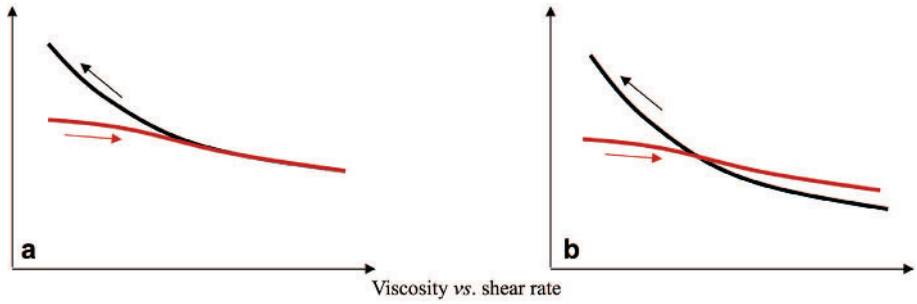

Figure 2. Hysteresis loops (viscosity *vs*. shear rate) types obtained in the present study: (a) when the shear acceleration was small; and (b) when the shear acceleration was large.

both cases the down curve exceeded the up curve in the low shear-rate region. To explain this result, the viscoelastic loop was examined (Greener and Connelly, 1986; Rubio-Hernández and Gómez-Merino, 2008). Using the Wagner model (Greener and Connelly, 1986) or the simpler Maxwell model (Rubio-Hernández and Gómez-Merino, 2008) to describe a viscoelastic material, a hysteresis loop with the same aspect as shown by kaolin suspensions at low shear rates are predicted theoretically. Based on these results, hysteresis loops at low shear rates should be due to the viscoelasticity of aqueous kaolin suspensions and not thixotropic behavior.

Specific tests designed to determine material functions that characterize the viscoelastic response of kaolin aqueous dispersions are, therefore, essential.

Viscoelastic behavior

An oscillating shear was applied to the material in order to achieve simultaneous information on its viscous and elastic components. Samples were subjected to an oscillating deformation

$$\gamma = \gamma_0 \sin\omega t \tag{4}$$

where γ_0 is the amplitude and ω is the angular frequency of the deformation. These two parameters control this type of test; two variants of the oscillating shear test can be defined as a result. If the frequency is fixed but the value of the amplitude of oscillation varies, an amplitude sweep test is applied to the sample. The aim of the amplitude sweep is to determine linear and non-linear viscoelastic behaviors. These two regions are separated by a critical amplitude value ($\gamma_{0_{max}}$). The procedure followed to obtain the critical amplitude value was as follows: the stress response to the oscillatory shear deformation given by equation 4 was, in general, out of phase by an amount, δ:

$$\tau = \tau_0 \sin(\omega t + \delta) \tag{5}$$

In equation 5, τ_0 is the amplitude of the shear stress. As the response of the material in the linear viscoelastic region is independent of the shear deformation amplitude, some functions of the material can be defined. Two of these are the storage (G') and loss (G'') moduli:

$$G' = \frac{\tau_0}{\gamma_0}\cos\delta$$
$$G'' = \frac{\tau_0}{\gamma_0}\sin\delta \tag{6}$$

The storage modulus expresses the elastic component of the shear stress, *i.e*. the part of the shear stress that is in phase with respect to the input deformation. In other words, G' is related to the energy stored in the dispersion. On the other hand, the loss modulus expresses the viscous component of the shear stress, *i.e*. the part of the shear stress that is phase shifted by 90º with respect to the input deformation, or in phase with respect to the shear rate ($\dot{\gamma} = \gamma_0\omega\cos\omega t$). In other words, G'' is related to the dissipation of energy in the dispersion.

The amplitude sweep applied to the samples, fixing the oscillation frequency, showed linear and non-linear viscoelastic regions (Figure 3). G' was greater than G'' when the amplitude of the oscillations was small. This was an expected result because small-amplitude oscillations demanded minor structure deformation and the system behaved essentially in linear 'solid-like' fashion. The values of loss and storage moduli were both constant up to a critical amplitude value. When the amplitude of the oscillation increased over the critical value, the strength of the structure diminished and both modulus values decreased. At greater oscillation amplitude, the viscous modulus dominated the elastic modulus and the material behaved in 'liquid-like' fashion. Another general observation was that both moduli increased when the dispersant concentration increased (Figure 3). This means that stronger microstructures were formed when the dispersant concentration increased.

The second oscillating shear test was defined by fixing the amplitude of the oscillation to a value which was less than the critical amplitude and then by varying the frequency of the oscillation. This is the frequency sweep test. The spectrum of frequencies allowed determination of the behavior of the material over short and long experimental times. The terms 'short' and 'long' refer to characteristic material times, which express the time required by the material to recover its rest configuration when distorted by an external

https://doi.org/10.1346/CCMN.2016.0640301 Published online by Cambridge University Press

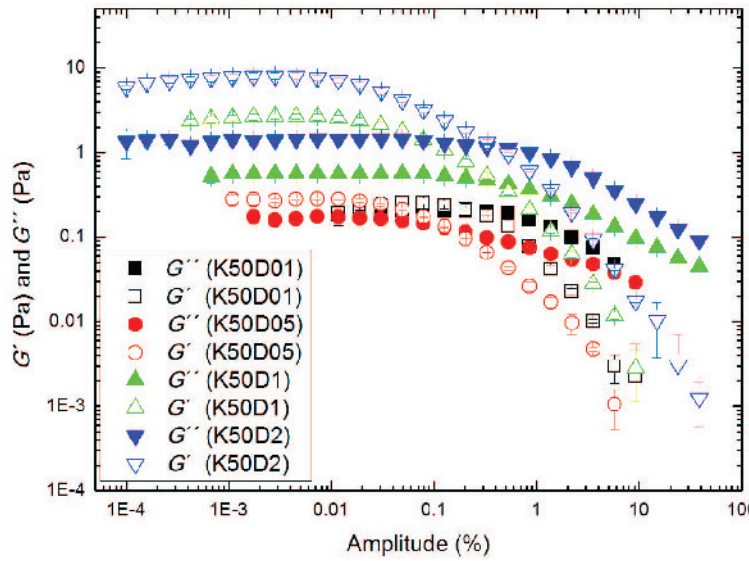

Figure 3. Results of the amplitude sweep. The frequency was fixed at 0.1 Hz in all cases.

mechanical action. This is known as the 'relaxation time.' To obtain the relaxation time of aqueous kaolin dispersions, frequency sweeps in the linear viscoelastic region are needed.

The results of the frequency sweep are shown in Figure 4. The terminal zone, *i.e.* where $G'(\omega)$ and $G''(\omega)$ follow simple Maxwell model predictions, was observed only with lower concentrations of dispersant. In this region of low frequencies, the dissipation modulus was greater than the storage modulus, *i.e.* the material behaved as a viscoelastic liquid. With increasing frequency, the storage modulus exceeded the loss modulus, *i.e.* the material behaved as a viscoelastic solid. This transition from viscoelastic liquid to viscoelastic solid is defined as the first characteristic frequency f_{c1} (Figure 4), which was only observed for the lower concentrations of dispersant, 0.100 and 0.500 wt.% (Table 4); the absence of the first characteristic frequency when dispersant concentration was >0.500 wt.% was an indication that the structure at rest in aqueous kaolin dispersions was elastic. The viscoelastic solid behavior (G'>G'') (Figure 4) persisted when the frequency increased until a second characteristic frequency value. The values of the second characteristic frequency (f_{c2}) obtained for each sample are shown in Table 4. This second frequency value marked the start of an instability region (non-reproducibility of the results).

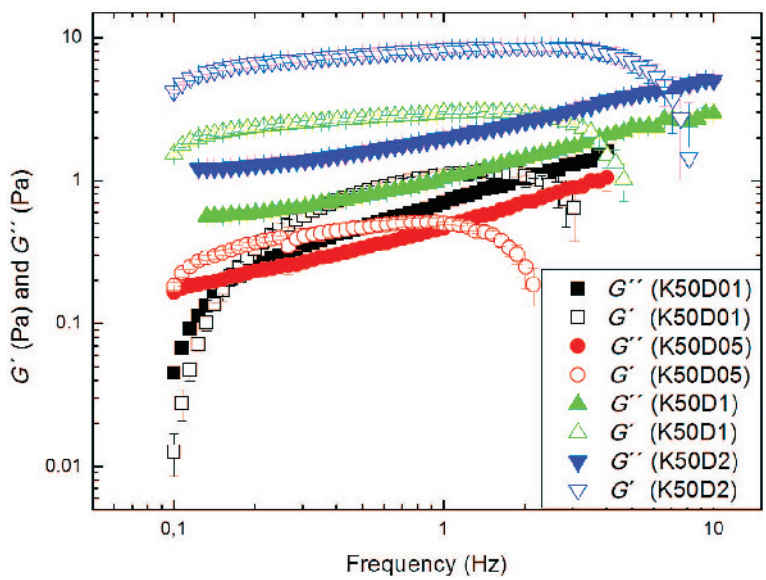

Figure 4. Results of the frequency sweep. The amplitude of the deformation was fixed at $\gamma_0 = 0.01$.

https://doi.org/10.1346/CCMN.2016.0640301 Published online by Cambridge University Press

Table 4. General analysis of the frequency sweeps. Values of the critical frequency for the transition from liquid-like to solid-like (f_{c1}) and the transition from solid-like to liquid-like (f_{c2}).

	NaHMP (wt.%)			
	0.100	0.500	1.000	2.000
f_{c1} (Hz)	0.18	0.10	–	–
f_{c2} (Hz)	2.0	2.5	3.5	7.1

To dispel the possibility that the second frequency might be due to instrumental artifacts, a frequency sweep was repeated with two different bob lengths. The results agreed within experimental error and so experimental artifacts are not the cause of the second characteristic frequency. The second characteristic frequency increased with dispersant concentration (Table 4). In other words, the dispersion was stable over a larger frequency interval when the dispersant concentration increased. This result opposes the prediction by Papo *et al.* (2002) who suggested that dispersant concentrations of >0.500 wt.% cause destabilization in aqueous kaolin dispersions stabilized with NaHMP. Moreover, both moduli were less dependent on the frequency in the medium-frequency region when dispersant concentration increased. This was also an indication of the formation of a stronger gel phase when NaHMP concentration increased above the critical limit of 0.500 wt.%.

A quantitative expression of solid-like behavior is the relaxation time of the elastic microstructure developed by kaolin particles. This parameter was obtained using the generalized Maxwell model for linear viscoelastic behavior. The model establishes a relationship (equation 7) between the shear-stress tensor ($\tilde{\tau}$) evaluated at current time (t) and the shear rate tensor ($\tilde{\dot{\gamma}}$) values at current and past times (t'),

$$\tilde{\tau}(t) = -\int_{-\infty}^{t}\left[\sum_{k=1}^{N}\left(\frac{\eta_k}{\lambda_k}\right)e^{-\frac{(t-t')}{\lambda_k}}\right]\tilde{\dot{\gamma}}(t')dt' \qquad (7)$$

This model assumes that the fluid is not characterized by a single relaxation time (λ), but rather that multiple relaxation times (λ_k) (where k represents the structure-structure level assumed) and a viscosity value (η_k) corresponding to each k-structure level are necessary to account for the whole relaxation process of the microstructure. The validity of this approach is supported by the Boltzmann superposition principle, *i.e.* the total stress is the sum of individual stresses due to each relaxation time (Morrison, 2001). The $2N$ parameters of the model, *i.e.* (η_k) and (λ_k) for k = 1 to N, supply sufficient flexibility to fit experimental frequency sweep curves. The generalized Maxwell model (equation 7) predicts the following dependence of storage and loss moduli with angular frequency:

$$\begin{aligned} G'(\omega) &= \sum_{k=1}^{N}\frac{g_k\lambda_k^2\omega^2}{1+\lambda_k^2\omega^2} \\ G''(\omega) &= \sum_{k=1}^{N}\frac{g_k\lambda_k\omega}{1+\lambda_k^2\omega^2} \end{aligned} \qquad (8)$$

where $g_k = \eta_k/\lambda_k$. A spreadsheet was used to fit the relaxation spectrum of the generalized Maxwell model to frequency sweep data obtained in the linear viscoelastic region (Table 5). To obtain the most representative relaxation time for each system, a weighted average was used:

Table 5. Maxwell's model parameters. Seven structural levels were sufficient in all cases to achieve valid fittings. Fitting was assumed to be valid when the objective function (Morrison, 2001) defined by

$$O = \sum_{i=1}^{M}\left\{\frac{\left[G'(\omega_i) - G'_{\text{model}}(\omega_i)\right]^2}{\left[G'(\omega_i)\right]^2} + \frac{\left[G''(\omega_i) - G''_{\text{model}}(\omega_i)\right]^2}{\left[G''(\omega_i)\right]^2}\right\}$$

was less than unity.

System	λ_1 (s)	λ_2 (s)	λ_3 (s)	λ_4 (s)	λ_5 (s)	λ_6 (s)	λ_7 (s)
K50D01	0.4	0.04	0.004	0.0004	0.00004	0.000004	0.0000004
K50D05	0.4	0.04	0.004	0.0004	0.00004	0.000004	0.0000004
K50D1	10	1	0.1	0.01	0.001	0.0001	0.00001
K50D2	1000	100	10	1	0.1	0.01	0.001

System	$g1$ (Pa)	$g2$ (Pa)	$g3$ (Pa)	$g4$ (Pa)	$g5$ (Pa)	$g6$ (Pa)	$g7$ (Pa)
K50D01	0.01	0.1	1	1	10	50	1000
K50D05	0.01	0.1	1	1	10	100	1000
K50D1	0.01	0.5	0.5	1	5	10	100
K50D2	0.9	1	1.5	2	3	4	5

https://doi.org/10.1346/CCMN.2016.0640301 Published online by Cambridge University Press

Table 6. Representative relaxation times (s). This parameter is the weighted average of the relaxation-time spectrum

System	λ
K50D01	0.022
K50D05	0.031
K50D1	0.060
K50D2	0.916

$$\lambda = \frac{\sum_{k=1}^{N} \lambda_k g_k}{\sum_{k=1}^{N} g_k} \quad (9)$$

The average relaxation time increased with the addition of dispersant (Table 6). This result agrees with the higher yield stress values observed when the concentration of the dispersant was increased. In other words, when NaHMP dispersant concentration increased above the critical value (0.500 wt.%), solid-like behavior was demonstrated by aqueous kaolin suspensions.

CONCLUSIONS

Aqueous kaolin dispersions using NaHMP showed viscoplastic behavior, which has not been reported previously, despite the important role that the yield stress plays in industrial applications. The addition of NaHMP dispersant in a concentration which was >0.500 wt.% reduced the yield-stress by three orders of magnitude. Frequency sweep tests in the region revealed a complex rheological behavior. At low and relatively high frequencies, the loss modulus was greater than the storage modulus, *i.e.* the system behaved in 'liquid-like' fashion. At medium frequencies, the storage modulus was greater than the loss modulus, *i.e.* the system behaved in 'solid-like' fashion, increasing the strength of the microstructure when dispersant concentration increased. Fitting G' and G'' moduli with the generalized viscoelastic Maxwell model, average relaxation times were obtained, which represent the softness of the solid-like structure developed by kaolin particles. This parameter increased with increasing concentration of the dispersant. The addition of NaHMP dispersant at a concentration >0.500 wt.% gave rise to more stable kaolin dispersions over time with increasing 'solid-like' behavior.

ACKNOWLEDGMENTS

FJRH is grateful for the grant (Becas Prometeo) received from the Secretaría Nacional de Educación Superior, Ciencia, Tecnología e Innovación (SENESCYT) Ecuador.

REFERENCES

Andreola, F., Castellini, E., Ferreira, J.M.F., Olhero, S., and Romagnoli M. (2006) Effect of sodium hexametaphosphate and ageing on the rheological behaviour of kaolin dispersions. *Applied Clay Science*, **31**, 56–64.

Barnes, H.A. (1999) The yield stress – a review or 'παντα ρει' – everything flows? *Journal of Non-Newtonian Fluid Mechanics*, **81**, 133–178.

Barnes, H.A., Hutton, J.F., and Walters K. (1989) *An Introduction to Rheology*. Elsevier Science Publishers, New York.

Bergaya, F., Theng, B.K.G., and Lagaly, G. (2006) *Handbook of Clay Science*. Elsevier, Amsterdam, pp. 502–506.

Choi, I.K., Went, W.W., and Smith, R.W. (1993) The effect of a long chain phosphate on the adsorption of collectors on kaolinite. *Minerals Engineering*, **6**, 1191–1197.

Eygi, M.S. and Ateşok, G. (2008) An investigation on utilization of poly-electrolytes as dispersant for kaolin slurry and its slip casting properties. *Ceramics International*, **34**, 1903–1908.

Feys, D., Verhoeven, R., and De Schutter, G. (2007) Evaluation of time independent rheological models applicable to fresh self-compacting concrete. *Applied Rheology*, **17**, 56244 (10 pp.).

Greener, J. and Connelly, R.W. (1986) The response of viscoelastic liquids to complex strain histories: the thixotropic loop. *Journal of Rheology*, **30**, 285–300.

Hunter, R.J. (1981) *Foundations of Colloid Science*. Academic Press, New York.

Konan, K.L., Peyratout, C., Cerbelaud, M., Smith, A., Bonnet, J.P., and Jacquet, A. (2008) Influence of two dispersants on the rheological behavior of kaolin and illite in concentrated calcium hydroxide dispersions. *Applied Clay Science*, **42**, 252–257.

Kronberg, B., Kuortti, J., and Stenius, P. (1986) Competitive and cooperative adsorption of polymers and surfactants on kaolinite surfaces. *Colloids and Surfaces*, **18**, 411–425.

Kwak, M.S., Ahn, H.J., and Song, K.W. (2015) Rheological investigation of body cream and body lotion in actual application conditions. *Korea-Australia Rheology Journal*, **27**, 241–251.

Le Bell, J.C., Hurskainen, V.T., and Stenius, P.J. (1976) The influence of sodium lignosulphonates on the stability of kaolin dispersions. *Journal of Colloid and Interface Science*, **55**, 60–68.

Li, Y., Zhang, Y., Zheng, J., Guo, H., Yang, C., Li, Z., and Lu, M. (2014) Dispersion and rheological properties of concentrated kaolin suspensions with polycarboxylate copolymers bearing comb-like side chains. *Journal of the European Ceramic Society*, **34**, 137–146.

Loginov, M., Larue, O., Lebovka, N., and Vorobiev, E. (2008) Fluidity of highly concentrated kaolin suspensions: Influence of particle concentration and presence of dispersant. *Colloids and Surfaces A*, **325**, 64–71.

Ma, M. (2011) The dispersive effect of sodium silicate on kaolinite particles in process water: implications for iron-ore processing. *Clays and Clay Minerals*, **59**, 233–239.

Manfredini, T., Pellacani, G.C., Pozzi, P., and Bonamartini Corradi, A. (1990) Monomeric and oligomeric phosphates as deflocculants of concentrated aqueous clay suspensions. *Applied Clay Science*, **5**, 193–201.

Mewis, J. and Spaull, A.J.B. (1976) Rheology of concentrated dispersions. *Advances in Colloid and Interface Science*, **6**, 173–200.

Morrison, F.A. (2001) *Understanding Rheology*. Oxford University Press, New York.

Murray, H.H. (1961) Industrial applications of kaolin. *Clays and Clay Minerals*, **10**, 291–298.

Murray, H.H. (2000) Traditional and new applications for kaolin, smectite, and palygorskite: a general overview. *Applied Clay Science*, **17**, 207–221.

Ouari, N., Kaci, A., Tahakourt, A., and Chaouche, M. (2011)

https://doi.org/10.1346/CCMN.2016.0640301 Published online by Cambridge University Press

Rheological behaviour of fibre suspensions in non-Newtonian fluids. *Applied Rheology*, **21**, 54801 (10 pp.).

Papo, A., Piani, L., and Ricceri, R. (2002) Sodium tripolyphosphate and polyphosphate as dispersing agents for kaolin suspensions: rheological characterization. *Colloids and Surfaces A*, **201**, 219–230.

Rand, B. and Melton, I.E. (1975) Isoelectric point of the edge surface of kaolinite. *Nature*, **257**, 214–216.

Rubio-Hernández, F.J. and Gómez-Merino, A.I. (2008) Time dependent mechanical behavior: the viscoelastic loop. *Mechanics of Time-Dependent Materials*, **12**, 357–364.

Schofield, R.K. and Samson, H.R. (1954) Flocculation of kaolinite due to the attraction of oppositely charged crystal faces. *Discussion Faraday Society*, **18**, 135–145.

Sjöberg, M., Bergström, L., Larsson, A., and Sjöström, E. (1999) The effect of polymer and surfactant adsorption on the colloidal stability and rheology of kaolin dispersions. *Colloids and Surfaces A*, **159**, 197–208.

Tombácz, E. and Szekeres, M. (2006) Surface charge heterogeneity of kaolinite in aqueous suspension in comparison with montmorillonite. *Applied Clay Science*, **34**, 105–124.

Triantafillopoulos, N.G. (1996) Paper Coating Viscoelasticity & its Significance in Blade Coating. TAPPI Press, UK.

Van Olphen, H. (1963) *An Introduction to Clay Colloid Chemistry*. Interscience, New York.

Van Olphen, H. (1964) Internal mutual flocculation in clay suspensions. *Journal of Colloid Science*, **19**, 313–322.

(*Received 22 May 2015; revised 24 March 2016; Ms. 1007; AE: Robert J. Pruett*)

https://doi.org/10.1346/CCMN.2016.0640301 Published online by Cambridge University Press